Phenoxyl, (Methylthio)phenoxyl, and (Methylthio)cresyl Radical Models for the Structures, Vibrations, and Spin Properties of the Cysteine-Linked Tyrosyl Radical in Galactose Oxidase

Kristopher E. Wise, J. Brett Pate, and Ralph A. Wheeler*

Department of Chemistry and Biochemistry, 620 Parrington Oval, Room 208, University of Oklahoma, Norman, Oklahoma 73019

Received: February 16, 1999; In Final Form: April 5, 1999

A cysteine-linked tyrosyl radical is implicated as a redox-active subunit in the stereospecific oxidation of D-alcohols to aldehydes by galactose oxidase. This contribution reports hybrid Hartree−Fock/density functional B3LYP/6-31G(d) quantum chemical calculations to compare the structures and properties of phenoxyl, (methylthio)phenoxyl, and (methylthio)cresyl radicals—increasingly accurate structural models for the biological radical. Calculated isotropic hyperfine coupling constants (hfcc's) for (methylthio)cresyl radical most closely resemble hfcc's measured for the apoenzyme (with Cu^{2+} removed), although the odd-alternant spin density pattern of phenoxyl radical is preserved in all three models. All three radicals are similarly accurate models for the vibrations of the enzyme's radical, although the calculated frequency for Wilson mode 19a, considered diagnostic for the cysteine-linked tyrosyl radical in galactose oxidase, appears closest to experimental results for the (methylthio)cresyl radical. Similarities between vibrational normal modes for the three radicals studied here are quantified by using a recently proposed comparative tool, vibrational projection analysis (Grafton, A. K.; Wheeler, R. A. *J. Comput. Chem.* **1998**, *19*, 1663; *Comput. Phys. Commun* **1998**, *113*, 78).

Amino acid radicals are believed to play essential roles in a number of vital enzymatic reactions.[1−7] Some of the most commonly encountered and most intensely studied amino acid radicals are the tyrosine phenoxyl radical and its derivatives. Derivatized tyrosine phenoxyl radicals, for example, have been identified in amine oxidases[8] and in galactose oxidase.[9,10] This work focuses on models for the radical detected in the latter system, a tyrosine phenoxyl radical covalently linked to a neighboring cysteine residue through a novel thioether bridge.

Galactose oxidase is a mononuclear copper enzyme composed of a single polypeptide (68 kDa molecular mass) that is folded into three domains. The enzyme catalyzes a remarkable reaction, the oxidation of primary alcohols to their corresponding aldehyde forms along with the coupled two-electron reduction of oxygen to hydrogen peroxide:[11,12]

$$RCH_2OH + O_2 \rightarrow RCHO + H_2O_2$$

Much attention has been devoted to galactose oxidase because of two fascinating features:[11,13] (1) it is a mononuclear metalloenzyme that catalyzes a two-electron redox process and (2) while galactose oxidase is relatively insensitive to the steric size of its substrates, it exhibits exclusive stereospecificity for D-isomers of the alcohols. This combination of features is unique to galactose oxidase and has generated intense interest in understanding the structure and function of its active site.

X-ray crystal structures of both the naturally occurring galactose oxidase metalloenzyme, its apoenzyme, and several mutant forms have been reported, allowing rapid advances in the understanding of how its active site functions.[3,13−15] As depicted in Figure 1, the active site is composed of a square-pyramidally coordinated Cu(II) center. The basal plane is occupied by two N-coordinated histidines (His496 and His581), an O-coordinated solvent molecule (acetate or water), and the

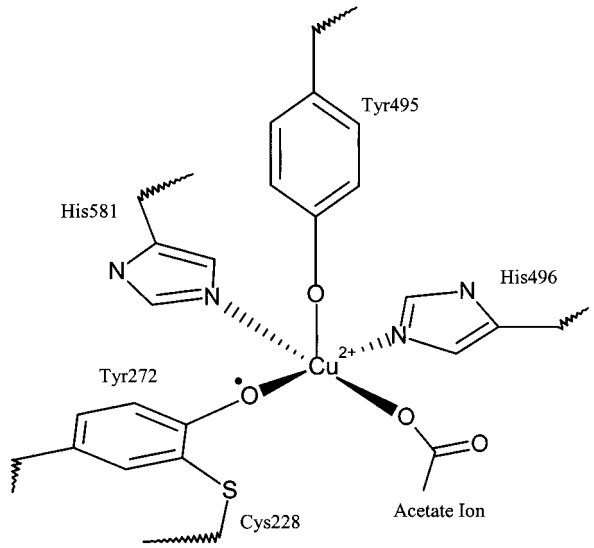

Figure 1. Schematic depiction of the copper coordination geometry in the active site of galactose oxidase. Placement of the radical symbol near the Tyr272 oxygen atom does not indicate spin localization.

O-coordinated tyrosine phenoxyl radical derivative (Tyr272). The ortho position of Tyr272 is the point of attachment for the unusual covalent sulfur linkage to the neighboring Cys228. The basal coordination of Cu is nearly perfectly planar, and the average metal−ligand distance is 2.1 Å.[14,15] The axial coordination position is occupied by another O-coordinated tyrosine (Tyr495) at a longer distance of 2.7 Å.

In addition to the structural characterization of this enzyme, extensive work has been reported detailing its electronic and vibrational spectra. In its activated form the metalloenzyme is found to be EPR-silent, despite the presence of two paramagnetic ($S = {}^1/_2$) species.[10,11,16] A high degree of antiferromagnetic

10.1021/jp990580q CCC: $18.00 © 1999 American Chemical Society
Published on Web 05/12/1999

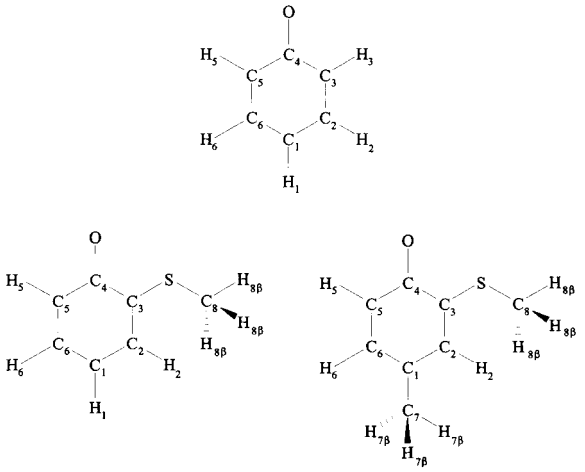

Figure 2. Phenoxyl radical (top), (methylthio)phenoxyl radical (bottom left), (methylthio)cresyl radical (bottom right). Figures illustrate connectivity and atom numbering only.

coupling between the Cu(II) center and the tyrosine phenoxyl radical is believed to be the reason.[10,11] By removing the copper center from the enzyme, Whittaker and co-workers were able to obtain partial EPR and ENDOR spectra of the organic radical species.[9,17] Estimates of the spin density distribution and of hyperfine coupling constants have been derived from these data and compared with a partial set of calculated values.[17] A primary conclusion drawn from comparing the experimental and computational work is that the tyrosine phenoxyl radical retains its odd-alternant spin density distribution with substantial spin density delocalization onto the cysteinyl sulfur. The spin and hyperfine properties of the model compounds studied in this work are compared with those available for the apoenzyme to evaluate their applicability in this essential area. Also included here are predicted values, from calculations on model systems, for the spin densities and hyperfine coupling constants that have not been determined experimentally for the apoenzyme.

Resonance Raman spectroscopy has been employed to obtain a partial vibrational spectrum of the radical species of interest.[18] This work allowed the assignment of C−O and C−C stretching and C−H bending bands. These data are used as an additional test of the applicability of the model compounds employed in our study. Further, our calculated vibrational data are used to affirm assignments for some of the ambiguous peaks in the experimental spectra of the azide adduct of galactose oxidase.[18]

The use of simplified models has traditionally been a valuable method for estimating the properties of more complex systems, particularly when the actual molecule of interest lies buried within a protein environment.[9,17−21] This approach is even more important when the species to be studied is not stable outside its protein environment, as is the case for the covalently modified tyrosine phenoxyl radicals involved in this work. Computational models have been employed successfully before, for example, to simulate the structures and properties of tyrosine phenoxyl radicals[22−27] and tryptophan indolyl radicals.[28−33] In this contribution, the calculated structures, spin properties, and vibrations of phenoxyl, (methylthio)phenoxyl, and (methylthio)-cresyl radicals, depicted in Figure 2, are reported and discussed. (It should be noted that the atom numbering scheme in Figure 2 differs from that traditionally used by organic chemists but was selected in accordance with the majority of publications describing tyrosyl radicals.) These three models of increasing similarity to the native tyrosine phenoxyl radical are compared to the available experimental data below, and not unexpectedly, the model most structurally similar to the biological radical, (methylthio)cresyl radical, is found to provide the best approximation to the native radical, both structurally and spectroscopically.

Molecular Structures

Owing to the very short lifetimes of most organic radicals, obtaining detailed information about their molecular structure is often impossible using traditional diffraction techniques. While amino acid radicals in proteins can be quite long-lived, the level of resolution of protein crystal structures is too coarse to allow for detailed, high-accuracy comparisons. For these reasons, computational methods have become essential sources of structural information about radicals and other transient species. In this paper the structures of phenoxyl, (methylthio)-phenoxyl (MTP$^\bullet$), and (methylthio)cresyl (MTC$^\bullet$) radicals are reported and the impact of incremental substitution is evaluated.

The description begins with the phenoxyl radical, which has been shown to be an excellent structural model for the tyrosine phenoxyl radical[23] and which provides a well-characterized baseline from which to explore the effects of thioether substitution. MTP$^\bullet$ is discussed next, as it is the simplest structural model for the novel thioether linkage between Cys228 and Y272 found in the galactose oxidase enzyme. Finally, the comparisons are concluded with MTC$^\bullet$, which includes both the thioether substituent at the position ortho to the phenoxyl oxygen and the methyl group in the para position to approximate the actual peptide chain. Although replacement of both Cys228 and the tyrosine backbone with methyl groups may seem like rather coarse approximations, it makes much higher accuracy calculations computationally feasible. More reliable predictions are obtained in this way than would be possible by using more complete models with less accurate methods.

The phenoxyl radical, the structural fragment common to all models considered in this work, has been studied previously using both uncorrelated (ROHF)[34] and correlated (CASSCF and UMP2) MO methods,[22,34] as well as by using a range of popular density functional methods.[18,22,25] The structural parameter most sensitive to the choice of method is the C−O bond length.[22] Calculated values range from that near a phenolic C−O single bond (1.38 Å from ROHF/3-21G)[34] to that of a more quinoidal C−O double bond (1.225 Å from UMP2/6-31G* and 1.228 Å from CASSCF/6-311G(2d,p)).[22,35] Values calculated using density functional theory (DFT) fall in the intermediate range 1.25−1.27 Å.[22,25] Unfortunately, no experimental structure has been reported for this radical, so assessing the accuracy of these disparate predictions is difficult.

The second column of Table 1 lists the results of a B3LYP/6-31G(d) calculation for phenoxyl radical. Comparison with the CASSCF results, listed in the first column, reveals excellent agreement for all bond lengths and angles except for the previously mentioned C−O bond length, which is found to be 0.030 Å longer than the CASSCF result. While normally very accurate, in this case some caution should be exercised in automatically accepting the CASSCF results as more accurate. This caution is warranted in light of reports that (1) increasing the size of the active space (in CASSCF calculations) tends to increase calculated C−O bond distances in related molecules[36] and (2) the dynamical correlation effects accounted for by DFT methods may be more important in this type of bonding situation than the nondynamical correlation contributions provided by CAS methods.[36] The overall agreement is, however, reassuring and gives a degree of confidence in going on to the substituted phenoxyl radicals below.

Having briefly reviewed the structure of the phenoxyl radical, the fundamental structural unit of these models, the structural

TABLE 1: Calculated Structures for Phenoxyl Radical, MTP•, and MTC•[a]

	phenoxyl[b]	phenoxyl[c]	MTP•[c]	MTC•[c]	MTC•[d]
			Bond Length (Å)		
C_1-C_2	1.411	1.410	1.396	1.401	
C_1-C_6	1.411	1.410	1.417	1.424	1.43
C_2-C_3	1.370	1.378	1.395	1.393	
C_6-C_5	1.370	1.378	1.372	1.369	1.38
C_4-C_3	1.454	1.453	1.473	1.471	
C_4-C_5	1.454	1.453	1.452	1.451	1.46
C_4-O	1.228	1.258	1.250	1.250	1.28
C_1-H_1	1.073	1.086	1.086		
C_2-H_2	1.074	1.087	1.085	1.085	
C_6-H_6	1.074	1.087	1.086	1.088	
C_3-H_3	1.073	1.086			
C_5-H_5	1.073	1.086	1.085	1.086	
C_3-S			1.750	1.752	1.78
$S-C_8$			1.824	1.824	1.87
C_8-H_{ip}			1.093	1.093	
C_8-H_{op}			1.093	1.094	
C_1-C_7				1.506	1.52
C_7-H_{ip}				1.094	
C_7-H_{op}				1.098	
			Bond Angle (deg)		
$C_2-C_1-C_6$	120.3	120.7	121.3	119.4	
$C_1-C_2-C_3$	120.6	120.2	120.3	121.3	
$C_1-C_6-C_5$	120.6	120.2	120.1	121.2	121.6
$C_3-C_4-C_5$	117.4	117.1	116.9	116.4	115.0
$C_4-C_3-C_2$	120.6	120.9	120.1	120.3	
$C_4-C_5-C_6$	120.6	120.9	121.3	121.5	122.2
C_3-C_4-O	121.3	121.4	120.9	121.1	
C_4-C_3-S			113.6	113.4	
C_3-S-C_8			102.6	102.7	
$C_2-C_1-C_7$				120.9	

[a] See Figure 2 for atom numbering. [b] Calculated using the CASSCF/6-311G(2d,p) method and basis set in ref 34. [c] Calculated using the B3LYP/6-31G(d) method and basis set in this work and ref 22. [d] Partial DFT calculated structure as reported in ref 17.

effects of ring substitution may now be examined, beginning with MTP•. The geometry of the phenoxyl ring of MTP•, listed in column three of Table 1, is seen to be significantly altered near the methylthio substituent group but nearly unchanged farther away from it. The immediately neighboring C_3-C_4 and C_2-C_3 bonds are longer by 0.020 and 0.017 Å, respectively, while the C_1-C_2 bond is shorter by 0.014 Å. On the other side of the ring the largest net change in bond distance is only 0.007 Å, indicating that any significant structural effects resulting from the substituent are somewhat localized to its immediate environment. A similarly small change (decrease of 0.007 Å) is found in the C_1-O bond distance.

Bond angles are less sensitive to substitution than bond distances, as is reflected in the small (all less than 1°) differences between phenoxyl radical and MTP•. The most significant changes are a 0.6° widening of the $C_2-C_1-C_6$ angle and a 0.8° narrowing of the $C_2-C_3-C_4$ angle, the location of the methylthio substituent. For both MTP• and MTC• (discussed below), the sulfur and carbon atoms of the methylthio substituent are perfectly coplanar with the ring. The minimum energy structure has the methyl group oriented away from the oxygen atom on the ring, although a second local minimum energy conformation at a slightly higher energy was found with the methyl group rotated toward the oxygen.

As might be expected, the geometrical changes induced by addition of a methyl group to MTP• are much smaller than those resulting from the addition of a thioether substituent to phenoxyl radical. The most significant changes in bond lengths occur in the C_1-C_2 and C_1-C_6 bonds, which are longer in MTC• than MTP• by 0.005 and 0.007 Å, respectively. All other ring C−C bonds are shorter by 0.001−0.003 Å, and the C_4-O distance is unchanged. Similarly minute changes are found in the thioether substituent. More significant angular changes are found, however. The $C_2-C_1-C_6$ angle is narrower by 1.9°, and the neighboring $C_1-C_2-C_3$ and $C_1-C_6-C_5$ angles are wider by 1.0° and 1.1°, respectively.

While structures have been reported for both MTP• and MTC• coordinated to copper complexes,[19−21] direct comparisons are not fruitful because of the large differences in bonding relative to the isolated radicals. A structure of the apogalactose enzyme has also been reported but the large uncertainties inherent in protein crystal structures limit the comparative value of this structure.[15] Finally, two other calculated structures for MTC• have been reported, one using the PM3 semiempirical method[21,37] and the other using a DFT method.[20] The DFT method used in the previous study, while including nonlocal corrections, does not account for the HF exchange energy. Inclusion of the HF exchange contribution as in the B3LYP method generally results in slightly more accurate calculated geometries.[36,38,39] The results of the aforementioned paper are, however, listed in column five of Table 1 for comparison. The longer C−O and C−S bond distances in published work apparently reflect the exclusion of the HF exchange contribution.

The structures of all three of these radicals show C−O bond lengths more similar to *p*-benzoquinone (1.225 Å)[40] than phenol (1.375−1.381 Å).[41,42] This quinoidal character is also shown in the C−C bond lengths, with the C_2-C_3 and C_5-C_6 bonds being markedly shorter than the others. Addition of the methylthio substituent results in moderate geometrical changes in its immediate vicinity but very small changes elsewhere in the ring system. The methyl group at the para position is seen to have a minimal influence. Finally, for both MTP• and MTC•, the methylthio substituent is found to prefer a coplanar arrangement with respect to the ring and an orientation with methyl away from the phenoxyl oxygen.

Spin Density Distributions and Hyperfine Coupling Constants

Electron spin resonance techniques (EPR, ENDOR, etc.) are invaluable for identifying and characterizing molecules with unpaired spins.[43,44] These species, which are usually transient in nature or buried in proteins, are normally difficult to probe with other spectroscopic or structural tools. In the case of galactose oxidase, for example, early studies revealed an EPR-silent active state.[10,11,16] Further work showed that once the copper center is removed from the enzyme, a spectrum characteristic of an odd-alternant tyrosine radical appears.[9,17] The absence of a signal prior to the removal of the Cu(II) atom is explained by invoking strong antiferromagnetic spin coupling between the metal center and a proximal amino acid radical, presumably tyrosine or some derivative.[10,11] Further work on the apoenzyme showed that the spectrum produced was not entirely consistent with the tyrosine phenoxyl radical. Some weakly coupling substituent appeared to have replaced an ortho proton on the phenoxyl ring. All of this work led to the insightful conclusions[9,10,18,19] that (1) a substituted tyrosine phenoxyl radical bears one of the two antiferromagnetically coupled electrons in the active site of the enzyme and (2) the substituent is actually a novel covalent thioether linkage to a neighboring cysteine residue.

As a second test of the ability of the models under study to approximate the properties of the tyrosyl residue in the apoenzyme, the spin densities and hyperfine coupling constants for all three models have been calculated. These results are

TABLE 2: B3LYP/6-31G(d) Calculated Spin Densities and Isotropic Hyperfine Coupling Constants (in gauss) for Phenoxyl Radical, MTP•, and MTC•

	spin densities				hyperfine coupling constants				
atom	phenoxyl	MTP•	MTC•	MTC•[a]	phenoxyl calcd	phenoxyl exptl[b]	MTP• calcd	MTC• calcd	exptl[c]
C_1	0.41	0.35	0.35	0.17	17.4		15.0	15.4	
C_2	−0.17	−0.16	−0.16	0.00	−10.1		−9.5	−9.6	
C_6	−0.17	−0.12	−0.11	0.04	−10.1		−7.6	−7.1	
C_3	0.32	0.28	0.28	0.16	12.7		12.4	12.3	
C_5	0.32	0.25	0.23	0.08	12.7		9.5	8.6	
C_4	−0.12	−0.06	−0.06	0.08	−11.5		−8.4	−7.9	
O	0.44	0.36	0.35	0.19	−11.8		−9.7	−9.6	
H_1	−0.02	−0.02			−9.7	10.2	−8.4		
H_2	0.01	0.01	0.01		3.1	1.9	2.9	2.8	0.3
H_6	0.01	0.00	0.00		3.1	1.9	2.1	1.7	0.5
H_3	−0.02				−7.7	6.6			
H_5	−0.02	−0.01	−0.01		−7.7	6.6	−6.1	−5.7	3.1
S		0.12	0.11	0.28			1.7	1.6	
C_8		−0.01	−0.01				−0.8	−0.7	
$H_{8\beta}$		0.00	0.00				1.9	1.8	1.7
C_7			−0.03					−3.9	
$H_{7\beta}$			0.01					9.0	8.6

[a] Subset of values from DFT calculations as reported in ref 17. [b] Reference 45. [c] Reference 21.

compared with experimental results where they are available, either from apogalactose oxidase or from model systems.[9,10,21] All calculated values are presented to assist in the interpretation or assignment of future experimental spectra. This work also provides an opportunity to study the extent of spin delocalization from the phenoxyl ring onto the methylthioether side chain. Since the sulfur and carbon atoms of this group are perfectly coplanar with the ring, it is reasonable to expect some degree of spin delocalization. As reported below, however, our calculations show only limited delocalization.

It is useful to begin the discussion with the simplest model system under consideration, the phenoxyl radical. The spin properties for this radical have already appeared in the literature,[22,23,45,46] so only a brief summary is given here. The phenoxyl radical shows a pronounced odd-alternant spin density distribution (Table 2) with the bulk of the unpaired spin located on the oxygen (0.41), ortho carbons (0.32), and para carbon (0.44). Experimental spin density ratios have been derived that show a para/ortho ratio of 1.5 and a para/meta ratio of 5.5.[45,46] B3LYP calculations reproduce the first ratio quantitatively (1.3) but the second only qualitatively (2.4). The proton hyperfine coupling constants (hfcc's), which are approximately proportional to the spin density on the adjacent heavy atom,[43,44] reflect this pattern as well. The magnitude of the ortho proton hfcc's (−7.7 G) are more than twice as large as the meta proton hfcc's (3.1 G), and the magnitude of the para proton hfcc (−9.7 G) is over 3 times as large. Again, these values compare well with experimentally determined magnitudes of 6.6, 1.9, and 10.2 G, respectively.[45] Only the magnitudes of the hfcc's have been experimentally determined; hence, the absolute value of the calculated hfcc's should be used for comparison purposes. Previous computational work has shown that careful modification of the basis set, particularly the core s-type orbital coefficients, can improve the results of hfcc calculations.[47] Basis sets of this type are not used here because functions for sulfur are not yet included in the basis sets.

Having discussed the spin structure of the parent phenoxyl radical, we now analyze the effect of methylthio functionalization. In the case of MTP• and MTC• one would expect some spin density delocalization from the ring to the methylthio substituent, and this is reflected both in experiment and in calculations. But either exocyclic substituent, the oxygen or the sulfur, may dictate the pattern of alternant spin densities for

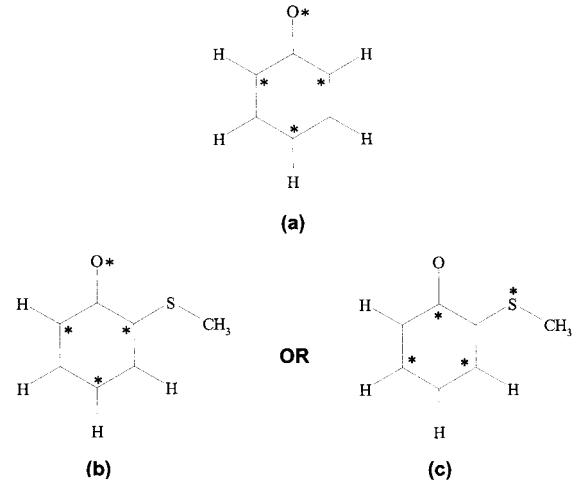

Figure 3. (a) Asterisks indicate locations of large spin densities on phenoxyl radical. (b,c) Asterisks indicate locations of large spin density populations for two limiting cases of alternant behavior for (methylthio)-phenoxyl radical (see Table 2).

MTP• and MTC• in the fashion illustrated in parts b and c of Figure 3. What has remained an open question, however, is whether Figure 3b or Figure 3c more accurately describes the extent of spin delocalization to the sulfur.

Experimental EPR work with other sulfur-containing radicals has shown that large orbital *g* shifts are found when a significant portion of the unpaired spin resides on the sulfur atom.[48,49] The importance of spin−orbit coupling in the valence region of sulfur has also been invoked to explain these shifts.[17] EPR studies of MTC• show that while the measured *g* values are different from those of unsubstituted phenoxyl radical, the methylthio substituent does not induce a dramatic change.[9,17] This result was originally taken to mean that little spin is delocalized onto the sulfur group in MTC•.[9] Later, in light of DFT calculations showing a large spin population on sulfur, the experimental data were reinterpreted and it was concluded that sulfur does, in fact, possess significant spin density. The authors proposed that mixing of the SOMO with low-lying unoccupied orbitals, rather than a small sulfur spin density, was responsible for the small change in *g* values.[17] The results presented below imply much less spin delocalization onto the sulfur than the recent DFT

calculations[17] and therefore appear more consistent with the first interpretation of the experimental data.[9]

The calculated spin density distributions (Table 2) for both MTP• and MTC• show the retention of an odd-alternant pattern on the ring and only moderate delocalization onto the sulfur, as indicated by Figure 3b. For MTP•, the only spin density value that has been confidently determined by ENDOR spectroscopy is for the para carbon, C_1, which is found to be 0.37,[9] in excellent agreement with the B3LYP calculated value of 0.35. The calculated spin densities on oxygen (0.36) and C_1 (0.35) decrease from their values in phenoxyl radical but are still 3 times as large as on the sulfur atom (0.12). Similarly, the spin densities on the ortho carbons of MTP•, C_3 (0.28) and C_5 (0.25), decrease relative to phenoxyl radical but remain twice as large as on sulfur. These results indicate that approximately 12% of the unpaired spin is transferred from the ring to the sulfur substituent. The addition of a methyl group at the para carbon position to form MTC• has an almost negligible impact on the spin density distribution. Inspection of Table 2 shows that the largest calculated change is only about 2% and only 1% on the sulfur atom (0.11). These results lead to the conclusion that the odd-alternate spin distribution found for the phenoxyl radical is retained in both MTP• and MTC•, with only a small amount of the spin density delocalized onto the neighboring sulfur atom.

Calculated isotropic proton hfcc's, which are approximately proportional to the spin density localized on the adjacent heavy atom, are expected to decrease in MTP• and MTC• from the corresponding values in the phenoxyl radical owing to the decrease in spin densities on the ring carbons. Table 2 shows this behavior, with the largest decreases in hfcc's between the phenoxyl radical and MTP• occurring at the H_1, H_6, and H_5 ring positions. Only minor changes in the hfcc's of the ring or methylthio group protons occur upon addition of the para methyl group, although the methyl protons couple strongly to unpaired spin on the ring. In the previous discussion of the phenoxyl radical hfcc's, it was seen the B3LYP/6-31G(d) method tended to slightly overestimate the ring proton hfcc's. This overestimation is seen again in the case of the MTC• hfcc's, particularly for the ring protons, although they do agree qualitatively with experimental results. Much better agreement is obtained for the methylthio protons (1.8 vs 1.7 G) and the para methyl protons (9.0 vs 8.6 G). It has been observed that the hyperfine interactions between the ring and the adjacent protons are much more anisotropic than the interactions of the methyl group protons,[9] which may explain why the calculated isotropic hfcc's for the methylthio and para methyl protons are in much better agreement with experimental values than are those for the ring protons.

It is well documented that the experimental high-frequency EPR spectra of MTC• and the radical species in the apogalactose oxidase enzyme are very similar.[9] The similarities in these spectra made it apparent that the radical species present in galactose oxidase is a covalently modified tyrosine phenoxyl radical, linked through an ortho carbon to a neighboring cysteine residue, as affirmed by X-ray crystallography.[3,13−15] The ability of the density functional method used in this study to reproduce the spin density and hyperfine coupling properties of MTC• accurately indicate its utility in future studies of this type and the applicability of MTC• as a good computational model for the electronic properties of the radical observed in galactose oxidase apoenzyme. The hfcc's reported here are also consistent with localization of spin density on the tyrosine−cysteine moiety of galactose oxidase, as suggested by Gerfen et al.,[17] rather than delocalization throughout a π-network incorporating a nearby tryptophan.

Vibrational Frequencies and Mode Assignments

Identification of the covalently modified tyrosine phenoxyl radical (Tyr272) as the radical-bearing species in galactose oxidase was reaffirmed by a recent resonance Raman study of the enzyme.[18] Galactose oxidase was previously known to absorb strongly from the UV to the near-IR spectral regions, but assignment of the transitions was made difficult by the number of chromophores in the vicinity of the active site.[50] Resonance Raman excitation of narrow spectral regions permitted observation and assignment of several strong frequencies that confirmed Tyr272 as the radical residue. In this section the calculated harmonic vibrational frequencies (see Table 3) are reported for MTP• and MTC• and assigned on the basis of their correlation with the previously described modes of the phenoxyl radical. Assignments listed in Table 3 include descriptions of the dominant atomic motions for each mode and, where appropriate, mode descriptions analogous to those suggested by Wilson for benzene.[51−53] Additionally, the available experimentally determined frequencies of the enzyme and of MTC• are compared with the calculated values, without scaling calculated frequencies. (Although some workers scale frequencies above ~1000 cm^{-1} by multiplying by 0.9614,[64] uniform frequency scaling actually worsens agreement between calculated frequencies for the model radicals and those measured for the radical in galactose oxidase.) For three modes, two experimental frequencies are listed in the table. The values listed first were measured in the galactose oxidase enzyme to which an azide ion had been added. Addition of azide is proposed to result in the displacement of the axial Tyr495 ligand from the copper center (see Figure 1) and to allow measurement of only the Tyr272 frequencies, albeit shifted by coordination to Cu^{2+}.[18] The second set of experimental frequencies given in the table are for the model compound MTC•, measured in a 0.1 M aqueous sodium hydroxide solution.

Since a number of workers have reported calculated frequencies and mode assignments for the parent phenoxyl radical,[22,25,34,35,54,55] only a short discussion will be given here. The method and basis set (B3LYP/6-31G(d)) used in this study were found to provide very accurate unscaled frequencies for the phenoxyl radical with an average absolute difference of only 22 cm^{-1} between results from calculations and nine experimentally measured frequencies and a maximum difference of 52 cm^{-1} for the CC stretching mode 8a.[22] Even much more expensive post-Hartree−Fock methods employing scaling factors are found to give only slightly better results.[22] The calculated mode assignments and corresponding harmonic frequencies are reported in the first two columns of Table 3. While the CC and CO stretching frequencies (phenoxyl radical's Wilson mode[51−53] 8a and 7a′, respectively) are very similar to those measured for galactose oxidase and the MTC• model, unscaled frequencies for the other ring modes differ by 23 cm^{-1} to almost 50 cm^{-1} from the galactose oxidase frequencies, with an average error of 26 cm^{-1}. These comparisons are consistent with the approximate error range expected for frequencies estimated by using B3LYP/6-31G(d) calculations for related radicals[22−24,28−30] and indicate the accuracy of using the phenoxyl radical to model the radical observed in galactose oxidase.

The effect of methylthio substitution is illustrated by comparing the phenoxyl and MTP• frequencies. For frequencies over

TABLE 3: Correlation of Phenoxyl Radical, MTP•, and MTC• B3LYP Calculated Harmonic Vibrational Frequencies (in cm^{-1})

mode description	phenoxyl	MTP•	MTC•	exptl
CH str	3222	3224	3218	
CH str	3220	3220		
CH str	3209	3203		
CH str	3194		3179/3203	
CH str	3187	3190	3203/3179	
C═C str (8a)	1603	1610	1623	1595[a]/1582[b]
CC str/CH bend	1564	1560	1483	
C−O str (7a′)	1499	1522	1558	1490[a]/1518[b]
CH bend/CC str (8b)	1458	1455	1465	1481[a]
CH bend/CC str (19a)	1433	1425	1422	1384[a]/1380[b]
CC str/CH bend	1352	1311	1307	1312[a,c]
CC str/CC bend (7a)	1289	1252	1266	1246[a,c]
CH bend/CC str	1176	1191	1020	
CH bend (9a)	1175	1150	1157	1185[a]
CH bend/CC str	1098			
CH bend/ring breath	1018	1039	1228	
HCCH tors	995	983	974/875	
CCC bend (18a)	986	1065	1068	
HCCH tors	975	937	875/974	
CH wag/boat def	922			
ring breath/CCC bend (1)	811	841	893/789	
CH wag	808	854		
chair def/CO wag	796	783	835	
chair def/CH wag	658	714	738	
CCC bend	598	662	665	
CCC bend (6a)	531	561	471	
boat def/CO wag	486	509	550	
CO bend	444	525	544	
ring def	381	438	442	
boat def/CO wag	196	252	312	
o-SMe CH str		3162	3160	
o-SMe CH str		3149	3147	
o-SMe CH str		3065	3064	
o-SMe CH bend		1513	1514	
o-SMe CH bend		1501	1501	
o-SMe CH bend		1390	1390	
o-SMe CH bend		1000	1003	
o-SMe CH bend		986	984	
o-SMe $S-C_{Me}$ str		720	721	
o-SMe $C_{rng}-S$ str/CCC bend		396	405	
o-SMe S bend/ring def			319	
o-SMe $C_{rng}-S-C_{Me}$ bend		271	268	
o-SMe CH wag		218	236	
o-SMe S bend		195	172	
o-SMe S bend/ring def			163	
o-SMe ring−S tors		130	122	
o-SMe Me wag		89	82	
p-Me CH str			3131	
p-Me CH str			3086	
p-Me CH str			3038	
p-Me CH bend			1526	
p-Me CH bend			1508	
p-Me CH bend			1441	
p-Me CH bend			1061	
p-Me CH bend			1020	
p-Me wag			60	

[a] Resonance Raman of galactose oxidase/azide adduct, ref 18. [b] Resonance Raman of MTC• in 0.1 M aqueous NaOH, ref 18. [c] Proposed assignment.

1000 cm^{-1} the largest calculated shift is −41 cm^{-1}, reflecting the influence of the substituent on the motions within the ring plane. In the lower frequency range, some out-of-plane torsional and wagging modes shift by 60−80 cm^{-1} and the ordering of several modes is changed. The much larger mass of the methylthio substituent compared to the hydrogen it replaces may be partially responsible for these shifts, but mode-mixing effects also contribute heavily.

The vibrational modes of the phenoxyl radical were quantitatively correlated with those of the more sophisticated models of MTP• and MTC• by using a method developed in this laboratory and briefly reviewed in the Appendix, vibrational projection analysis.[56,57] Vibrational projection analysis simply projects the orthonormal set of vectors comprising a molecule's normal modes onto the normal modes of a second, related molecule. The similarity of the vector representations of the vibrational modes of the two molecules allows for a quantitative, objective correlation of the two sets of calculated frequencies. This method greatly reduces the time required to correlate two sets of vibrational modes while decreasing the chances of making incorrect pairings. Included as Supporting Information (Tables S1−S3) are the results of the three vibrational projection analyses used in this work. These tables contain mode correlations of MTP• with phenoxyl radical, MTC• with phenoxyl radical, and MTC• with MTP•, respectively.

Matching calculated modes of phenoxyl radical and MTP• clearly shows the power of vibrational projection analysis (ViPA) to deconvolute mode mixing. For example, the experimentally detected Wilson mode 8a, a CC stretch, was calculated at 1603 cm^{-1} for the phenoxyl radical, and the corresponding mode of MTP•, calculated to appear at 1610 cm^{-1}, consists of 81% phenoxyl mode 8a (see Table S3 in Supporting Information). Similarly, the MTP• Wilson modes 19a (considered diagnostic of the cysteine-linked tyrosyl radical[18]) and 7a each correlate rather unambiguously with a single mode of the phenoxyl radical. Vibrational projection analysis is perhaps most useful, however, for clarifying ambiguous cases of mode mixing. According to ViPA, the CO stretch of MTP•, calculated to appear at 1522 cm^{-1}, consists of almost equal amounts of phenoxyl CO stretching and CC stretching/CH bending modes. Likewise, the MTP• mode (at 1560 cm^{-1}), labeled as CC stretching/CH bending in Table 3, consists of a nearly equal mixture of the same two phenoxyl modes. Rather than making an absolute statement about the composition of these modes, ViPA allows a more precise correlation of phenoxyl radical modes with those of MTP•.

Comparing the calculated and measured frequencies shows that several calculated MTP• frequencies appear closer than the corresponding phenoxyl radical frequencies to the measured frequencies of the radical in galactose oxidase, but only two MTP• frequencies—calculated at 1311 and 1252 cm^{-1}—appear significantly closer. It should also be noted that three pairs of C−H modes (two stretches at 3209 and 3194 cm^{-1}, two bends at 1175 and 1098 cm^{-1}, and two wags at 975 and 922 cm^{-1}) in the phenoxyl radical are replaced by three single C−H modes (3203, 1150, and 937 cm^{-1}) and three new interfragment modes ($C_6H_4O-SCH_3$) in MTP• owing to the replacement of a hydrogen with the methylthio group. The new substituent modes (labeled *o*-SMe) are reported and assigned below the phenoxyl modes in Table 3. Differences between calculated and experimentally measured frequencies are probably due to a combination of errors due to the B3LYP/6-31G(d) method and environmental effects present in the experimental measurements, especially coordination to Cu^{2+}, that are not accounted for in these calculations.

The calculated frequencies for MTC• show features similar to those described above. Modest improvements in agreement between calculated and experimental frequencies are found for several modes composed of C−H bending and C−C stretching contributions such as 8b and the important 19a mode. A moderate shift of the CC stretching frequency for Wilson mode 8a (from 1610 cm^{-1} in MTP• to 1623 cm^{-1} in MTC•) and a larger shift in the CO stretching frequency (from 1522 cm^{-1} in MTP• to 1558 cm^{-1} for MTC•) give poorer agreement between

calculations and experiment for MTC• than for MTP•. Finally, the nine new substituent modes, labeled *p*-Me, are reported and assigned at the end of Table 3.

While the average errors between experimental frequencies for the cysteine-linked tyrosyl radical in galactose oxidase and those calculated for the three model systems are relatively small and similar (26, 22, and 27 cm^{-1} for phenoxyl, MTP•, and MTC•, respectively), there are some important differences, particularly for the diagnostic 19a mode and the important CO stretching mode 7a′. The 19a mode of MTC• is calculated to appear closest to the frequency measured for the cysteine-linked tyrosyl radical in galactose oxidase, whereas Cu^{2+} coordination to the oxygen atom of the cysteine-linked tyrosyl radical probably causes a significant shift of the CO stretching mode to lower frequencies in the enzyme. In summary then, it appears that MTC• is only a slightly better model than the MTP• and phenoxyl radicals for the vibrations of the cysteine-linked tyrosyl radical in galactose oxidase.

Conclusions

Model studies, both experimental and computational, are an invaluable means of gaining information about transient or otherwise inaccessible species. This work reports the most complete set of computational results characterizing the (methylthio)phenoxyl radical (MTP•) and the (methylthio)cresyl radical (MTC•) currently available, including structures, spin densities, hyperfine coupling constants, and harmonic vibrational frequencies and mode assignments.

Structurally, addition of the methylthio functional group at the ortho position of the phenoxyl radical parent molecule is found to have a moderate effect on the ring C−C bond lengths proximal to the substituent, resulting in bond length changes of approximately 0.02 Å, and smaller effects on other bond distances. Addition of a methyl group at the para position has a minimal impact on the ring geometry. The methylthio substituent is found to prefer a coplanar orientation with respect to the ring with the terminal methyl group aimed away from the phenoxyl oxygen, in accordance with the crystal structure of galactose oxidase.

Calculated spin densities confirm that the odd-alternant spin pattern found in the phenoxyl radical is retained upon addition of both the *o*-methylthio and *p*-methyl substituents. Only about 12% of the total unpaired spin is calculated to be delocalized onto the sulfur atom, indicating that the phenoxyl ring is the primary host for the odd electron. These findings are consistent with experimental results but show less spin delocalization to sulfur than previous calculations. The calculated hyperfine coupling constants compare well with experimental measurements, particularly for the two sets of methyl protons in MTC•, which are in error by only about 5%.

Finally, the calculated harmonic vibrational frequencies for MTC• show an average absolute difference from the seven experimentally reported values of only 27 cm^{-1}. Frequencies for the MTP• and phenoxyl radical are also very close to experimental values, with an average absolute difference of 22 and 26 cm^{-1}, respectively. The vibrational frequency for the Wilson mode 19a, considered diagnostic for the cysteine-linked tyrosyl radical in galactose oxidase,[18] is closest for MTC• to the experimentally measured frequency, whereas the CO stretching mode's frequency for MTC• is much higher than the experimental value. The discrepancy between calculated and experimental CO stretching frequencies may be due to Cu^{2+} coordination to the radical's oxygen in galactose oxidase. Correlations between calculated vibrational modes for the different radicals (phenoxyl radical, MTC•, and MTP•) were made using a simple yet powerful technique called vibrational projection analysis.[56,57] The complete listing of calculated frequencies and the correlation of mode assignments among phenoxyl radical, MTP•, and MTC• are reported as Supporting Information for use in future assignments of experimental spectra and to clarify differences in vibrational frequencies inherent in the MTC•, MTP•, and phenoxyl radical models.

In summary, calculations indicate that MTC• is the best overall model for the native, covalently modified tyrosyl radical observed in galactose oxidase, of the three models studied here. MTP• also performs well, but removal of the methylthio functionality, leaving the phenoxyl radical, results in a model incapable of reproducing many important structural, spin, and hyperfine properties of the native species.

Acknowledgment. We are grateful for supercomputer time at the University of Oklahoma made possible by support from IBM Corporation (in part through a Shared University Research grant), Silicon Graphics, Inc., and the University of Oklahoma. K.E.W. also thanks Dr. Anthony K. Grafton for providing early access to his vibrational analysis program ViPA and for helpful discussions on its usage.

Appendix: Computational Methods

All B3LYP[58] calculations of structures, vibrational frequencies, and spin densities reported in this work were performed with the GAUSSIAN94[59] program package using a 6-31G(d) basis set[60] and the standard integration grid. Geometries were optimized using Berny's optimization algorithm[61] without symmetry restriction. Harmonic vibrational frequency calculations were performed for each optimized structure. Spin densities were calculated using Mulliken population analysis.[62] The Fermi contact term for each atom (ρ_N) was used to calculate the corresponding isotropic hyperfine coupling constant according to the equation

$$a_o = \{(8\pi/3)g_E g_N \beta_E \beta_N\}\rho_N$$

where g_E is the electronic g factor, β_E is the electronic Bohr magneton, and g_N and β_N are the corresponding values for each nucleus.

Vibrational normal modes for the various radicals were compared in pairs by using the recently developed vibrational projection analysis (ViPA) method.[56,57] Our computer program for vibrational projection analysis[56,57] assesses the similarity of mass-weighted Cartesian displacement coordinates, i.e., vibrational normal modes, between an object molecule and a related basis molecule using vector projections. The program begins by aligning the two molecules and converting the Cartesian force constant matrix produced by the electronic structure program to a mass-weighted Cartesian force constant matrix ($\underline{\underline{F}}$). The matrix is diagonalized using the Jacobi method,[63] and the result is a set of $3N$ eigenvectors $\underline{A}$, the normal modes, and a set of $3N$ eigenvalues proportional to the vibrational frequencies. Each of the N eigenvectors, $\mathbf{A}_j$, is a $3N \times 1$ column vector that is orthonormal to all other members of $\underline{A}$. The procedure is repeated for molecule 2, the object molecule, to find a set of $3N'$ normal modes ($N' \geq N$), which are also orthonormal column vectors, labeled $\mathbf{B}_k$, of dimension $3N' \times 1$. With these two sets of vectors, $\mathbf{A}_j$ of the basis molecule and $\mathbf{B}_k$ of the object

molecule, the vector projection operation is done by sequentially projecting each eigenvector $\mathbf{B}_k$ of the object molecule onto each eigenvector $\mathbf{A}_j$ of the basis molecule:

$$\mathbf{B}_k^{\mathrm{T}}\mathbf{A}_j = c_{kj}$$

The result of each projection, c_{kj}, constitutes an element of a new matrix, $\underline{\underline{C}}$, of dimension $3N \times 3N'$. The sum of the squares of the elements c_{kj} over all $3N$ modes is equivalent to the norm of vector $\mathbf{B}_k$ projected onto the orthonormal vector space of $\underline{A}$. Therefore, the value c_{kj}^2 is a measure of the similarity of a given mode k of the object molecule to the modes j of the basis molecule. Multiplication of c_{kj}^2 by 100 expresses this similarity as a percentage.

The output of the program lists each normal mode of the object molecule and gives the percentage contribution that each normal mode of the basis molecule makes to it. So for a mode k of the object molecule, each of the $3N$ modes of the basis molecule is listed along with their respective percentage contribution, ranging from 0, for no contribution, to 100 for an identical match. Summing the percentage contributions down the column yields a total of 100% if the basis molecule's normal modes are a perfect representation of that particular mode of the object molecule. Since the object and basis molecules are not identical, there is often some percentage of the object molecule's mode that cannot be accounted for by the basis molecule. In these cases a deficit, or d-factor, is reported as

$$d_{kj}^{\%} = 100 - \sum c_{kj}^{\%}$$

A small value of the d-factor indicates that the particular mode of the object molecule is well represented by the modes of the basis molecule, and a large value indicates that the particular mode is not well represented as a combination of basis molecule modes. Output from this program discussed in the text is provided in the Tables S1−S3 of Supporting Information.

Supporting Information Available: Three tables showing vibrational projection analysis relating the normal modes of (methylthio)phenoxyl radical, (methylthio)cresyl radical, and phenoxyl radical. This material is available free of charge via the Internet at http://pubs.acs.org.

References and Notes

(1) Stubbe, J. A.; van der Donk, W. A. *Chem. Rev.* **1998**, *98*, 705−762.

(2) Easton, C. J. *Chem. Rev.* **1997**, *97*, 53−82.

(3) Ito, N.; Knowles, P. F.; Phillips, S. E. V. *Methods Enzymol.* **1995**, *258*, 235−262.

(4) *Metal Ions in Biological Systems, Volume 30: Metalloenzymes Involving Amino-Acid Residues and Related Radicals*; Sigel, H., Sigel, A., Eds.; Marcel Dekker: New York, 1994.

(5) Pedersen, J. Z.; Finazzi-Agro, A. *FEBS Lett.* **1993**, *325*, 53−58.

(6) Stadtman, E. R. *Annu. Rev. Biochem.* **1993**, *62*, 797−821.

(7) Stubbe, J. A. *Annu. Rev. Biochem.* **1989**, *58*, 257−285.

(8) Janes, S. M.; Mu, D.; Wemmer, D.; Smith, A. J.; Kaus, S.; Maltby, D.; Burlingame, A. L.; Klinman, J. P. *Science* **1990**, *248*, 981−987.

(9) Babcock, G. T.; El-Deeb, M. K.; Sandusky, P. O.; Whittaker, M. M.; Whittaker, J. W. *J. Am. Chem. Soc.* **1992**, *114*, 3727−3734.

(10) Whittaker, M. M.; Whittaker, J. W. *J. Biol. Chem.* **1990**, *265*, 9610−9613.

(11) Whittaker, M. M.; Whittaker, J. W. *J. Biol. Chem.* **1988**, *263*, 6074−6080.

(12) Tressel, P. S.; Kosman, D. J. *Methods Enzymol.* **1982**, *89*, 163.

(13) Baron, A. J.; Stevens, C.; Wilmot, C.; Seneviratne, K. D.; Blakely, V.; Dooley, D. M.; Phillips, S. E. V.; Knowles, P. F.; McPherson, M. J. *J. Biol. Chem.* **1994**, *269*, 25095−25105.

(14) Ito, N.; Phillips, S. E. V.; Stevens, C.; Ogel, Z. B.; McPherson, M. J.; Keen, J. N.; Yadav, K. D. S.; Knowles, P. F. *Nature* **1991**, *350*, 87−90.

(15) Ito, N.; Phillips, S. E. V.; Yadav, K. D. S.; Knowles, P. F. *J. Mol. Biol.* **1994**, *238*, 794−814.

(16) Hamilton, G. A.; Adolf, P. K.; de Jersey, J.; DuBois, G. C.; Dyrkacz, G. R.; Libby, R. D. *J. Am. Chem. Soc.* **1978**, *100*, 1899−1912.

(17) Gerfen, G. J.; Bellew, B. F.; Griffin, R. G.; Singel, D. J.; Ekberg, C. A.; Whittaker, J. W. *J. Phys. Chem.* **1996**, *100*, 16739−16748.

(18) McGlashen, M. L.; Eads, D. D.; Spiro, T. G.; Whittaker, J. W. *J. Phys. Chem.* **1995**, *99*, 4918−4922.

(19) Whittaker, M. M.; Chuang, Y. Y.; Whittaker, J. W. *J. Am. Chem. Soc.* **1993**, *115*, 10029−10035.

(20) Whittaker, M. M.; Duncan, W. R.; Whittaker, J. W. *Inorg. Chem.* **1996**, *35*, 382−386.

(21) Itoh, S.; Takayama, S.; Arakawa, R.; Furuta, A.; Komatsu, M.; Ishida, A.; Takamuku, S.; Fukuzumi, S. *Inorg. Chem.* **1997**, *36*, 1407−1416.

(22) Qin, Y.; Wheeler, R. A. *J. Chem. Phys.* **1995**, *102*, 1689−1698.

(23) Qin, Y.; Wheeler, R. A. *J. Am. Chem. Soc.* **1995**, *117*, 6083−6092.

(24) Qin, Y.; Wheeler, R. A. *J. Phys. Chem.* **1996**, *100*, 10554−10563.

(25) Nwobi, O.; Higgins, J.; Zhou, X.; Liu, R. *Chem. Phys. Lett.* **1997**, *272*, 155−161.

(26) Himo, F.; Graslund, A.; Eriksson, L. A. *Biophys. J.* **1997**, *72*, 1556.

(27) O'Malley, P. J.; Ellson, D. *Biochim. Biophys. Acta* **1997**, *1320*, 65.

(28) Walden, S. E.; Wheeler, R. A. *J. Phys. Chem.* **1996**, *100*, 1530−1535.

(29) Walden, S. E.; Wheeler, R. A. *J. Chem. Soc., Perkin Trans. 2* **1996**, 2663−2672.

(30) Walden, S. E.; Wheeler, R. A. *J. Am. Chem. Soc.* **1997**, *119*, 3175−3176.

(31) Lendzian, F.; Sahlin, M.; MacMillan, F.; Bittl, R.; Fiege, R.; Potsch, S.; Sjoberg, B.-M.; Graslund, A.; Lubitz, W.; Lassmann, G. *J. Am. Chem. Soc.* **1996**, *118*, 8111.

(32) Jenson, G. M.; Goodin, D. B.; Bunte, S. W. *J. Phys. Chem.* **1996**, *100*, 954.

(33) O'Malley, P. J.; Ellson, D. A. *Chem. Phys. Lett.* **1996**, *260*, 492.

(34) Chipman, D. M.; Liu, R.; Zhou, X.; Pulay, P. *J. Chem. Phys.* **1994**, *100*, 5023−5035.

(35) Liu, R.; Zhou, X. *Chem. Phys. Lett.* **1993**, *207*, 185−189.

(36) Adamo, C.; Barone, V.; Fortunelli, A. *J. Chem. Phys.* **1995**, *102*, 384−393.

(37) Itoh, S.; Hirano, K.; Furuta, A.; Komatsu, M.; Ohshiro, Y.; Ishida, A.; Takamuku, S.; Kohzuma, T.; Nakamura, N.; Suzuki, S. *Chem. Lett.* **1993**, 2099−2102.

(38) Lelj, F.; Adamo, C.; Barone, V. *Chem. Phys. Lett.* **1994**, *230*, 189−195.

(39) Barone, V. *Chem. Phys. Lett.* **1994**, *226*, 392−398.

(40) Hagen, K.; Hedberg, K. *J. Chem. Phys.* **1973**, *59*, 158−162.

(41) Portalone, G.; Schultz, G.; Domenicano, A.; Hargittai, I. *Chem. Phys. Lett.* **1992**, *197*, 482−488.

(42) Larsen, N. W. *J. Mol. Struct.* **1979**, *51*, 175−190.

(43) Gordy, W. *Theory and Applications of Electron Spin Resonance*; Wiley-Interscience: New York, 1980.

(44) Weil, J.; Bolton, J. R.; Wertz, J. E. *Electron Paramagnetic Resonance*; Wiler-Interscience: New York, 1994.

(45) Neta, P.; Fessenden, R. W. *J. Phys. Chem.* **1974**, *78*, 523−529.

(46) Stone, T. J.; Waters, W. A. *J. Chem. Soc.* **1964**, 213−218.

(47) Chipman, D. *Theor. Chim. Acta* **1989**, *76*, 73−84.

(48) Box, H. C.; Budzinski, E. E. *J. Chem. Soc., Perkins Trans. 2* **1976**, 553−555.

(49) Preston, K. F.; Sutcliffe, L. H. *Magn. Reson. Chem.* **1990**, *28*, 189−204.

(50) Whittaker, M. M.; DeVito, V. L.; Asher, S. A.; Whittaker, J. W. *J. Biol. Chem.* **1989**, *264*, 7104−7106.

(51) Wilson, E. B. *Phys. Rev.* **1934**, *45*, 706−714.

(52) Varsanyi, G. *Vibrational Spectra of Benzene Derivatives*; Academic Press: New York, 1969.

(53) Dollish, F. R.; Fateley, W. G.; Bentley, F. F. *Characteristic Raman Frequencies of Organic Compounds*; Wiley-Interscience: New York, 1974.

(54) Tripathy, G. N. R.; Schuler, R. H. *J. Phys. Chem.* **1988**, *92*, 5129−5133.

(55) Mukherjee, A.; McGlashen, M. L.; Spiro, T. G. *J. Phys. Chem.* **1995**, *99*, 4912.

(56) Grafton, A. K.; Wheeler, R. A. *J. Comput. Chem.* **1998**, *19*, 1663−1674.

(57) Grafton, A. K.; Wheeler, R. A. *Comput. Phys. Commun.* **1998**, *113*, 78−84.

(58) Becke, A. D. *J. Chem. Phys.* **1993**, *98*, 5648−5652.

(59) Frisch, M. J.; Trucks, G. W.; Schlegel, H. B.; Gill, P. M. W.; Johnson, B. G.; Robb, M. A.; Cheeseman, J. R.; Keith, T. A.; Petersson, G. A.; Montgomery, J. A.; Raghavachari, K.; Al-Laham, M. A.; Zakrzewski, V. G.; Ortiz, J. V.; Foresman, J. B.; Peng, C. Y.; Ayala, P. A.; Wong, M. W.; Andres, J. L.; Replogle, E. S.; Gomperts, R.; Martin, R. L.; Fox, D. J.; Binkley, J. S.; Defrees, D. J.; Baker, J.; Stewart, J. P.; Head-Gordon, M.; Gonzalez, C.; Pople, J. A. *GAUSSIAN94*, revisions B2, B3, D1, and D2; Gaussian, Inc.: Pittsburgh, PA, 1995.

(60) Hehre, W. J.; Radom, L.; Schleyer, P. V. R.; Pople, J. A. *Ab Initio Molecular Orbital Theory*; Wiley: New York, 1986.

(61) Schlegel, H. B. *J. Comput. Chem.* **1982**, *3*, 214−218.

(62) Mulliken, R. S. *J. Chem. Phys.* **1955**, *23*, 1833−1840.

(63) Press, W. H.; Flannery, B. P.; Teukolsky, S. A.; Vetterling, W. T. *Numerical Recipies, The Art of Scientific Computing*; Cambridge University Press: Cambridge, 1987.

(64) Scott, A. P.; Radom, L. *J. Phys. Chem.* **1996**, *100*, 16502−16513.